

Supplementary Materials for  
**Real-time monitoring of drug pharmacokinetics within  
tumor tissue in live animals**

Ji-Won Seo, Kaiyu Fu, Santiago Correa, Michael Eisenstein, Eric A. Appel\*, Hyongsok T. Soh\*

\*Corresponding author. Email: [eappel@stanford.edu](mailto:eappel@stanford.edu) (E.A.A.); [tsoh@stanford.edu](mailto:tsoh@stanford.edu) (H.T.S.)

Published 7 January 2022, *Sci. Adv.* **8**, eabk2901 (2022)  
DOI: 10.1126/sciadv.abk2901

**This PDF file includes:**

Figs. S1 to S11  
Table S1

## Supporting information

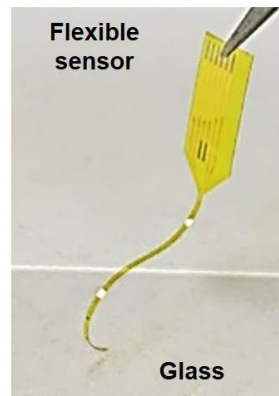


**Figure S1. Flexible polyimide-based sensor on glass.** The probe is shaped to minimize damage at the site of insertion, and offers a good match to the physical properties of surrounding tissue. Photo Credit: Ji-Won Seo, Stanford University.

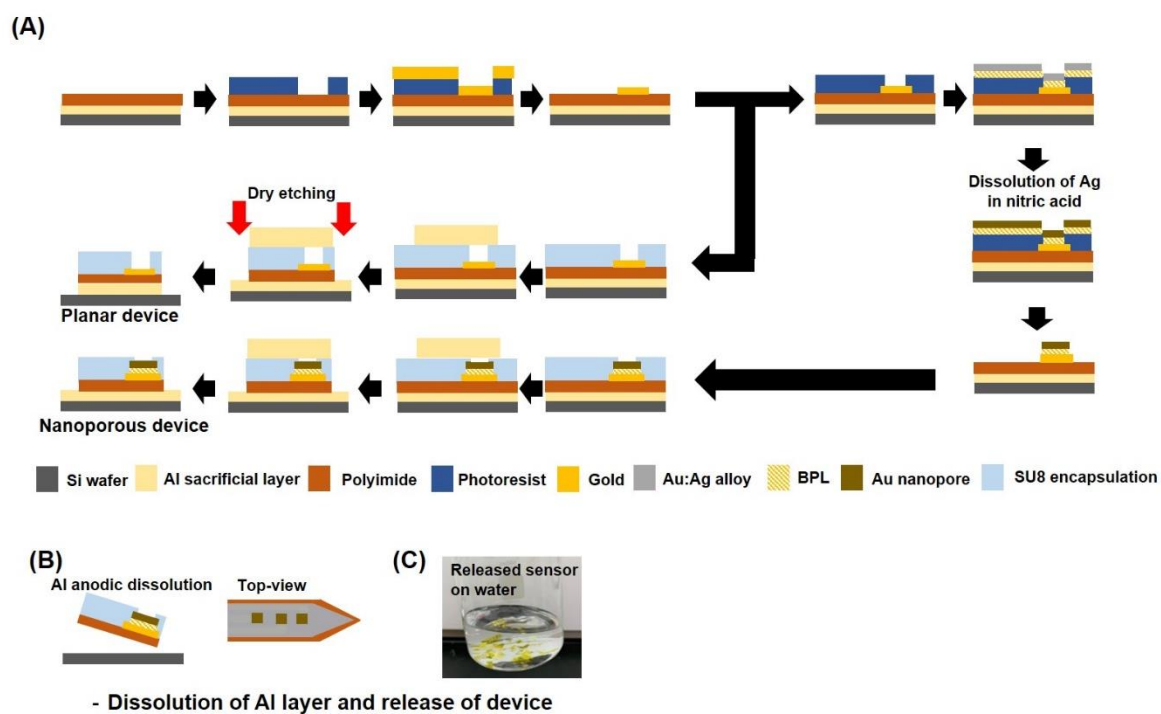


**Figure S2. Schematic illustration of the fabrication process of gold nanoporous and planar microelectrode array sensor.**

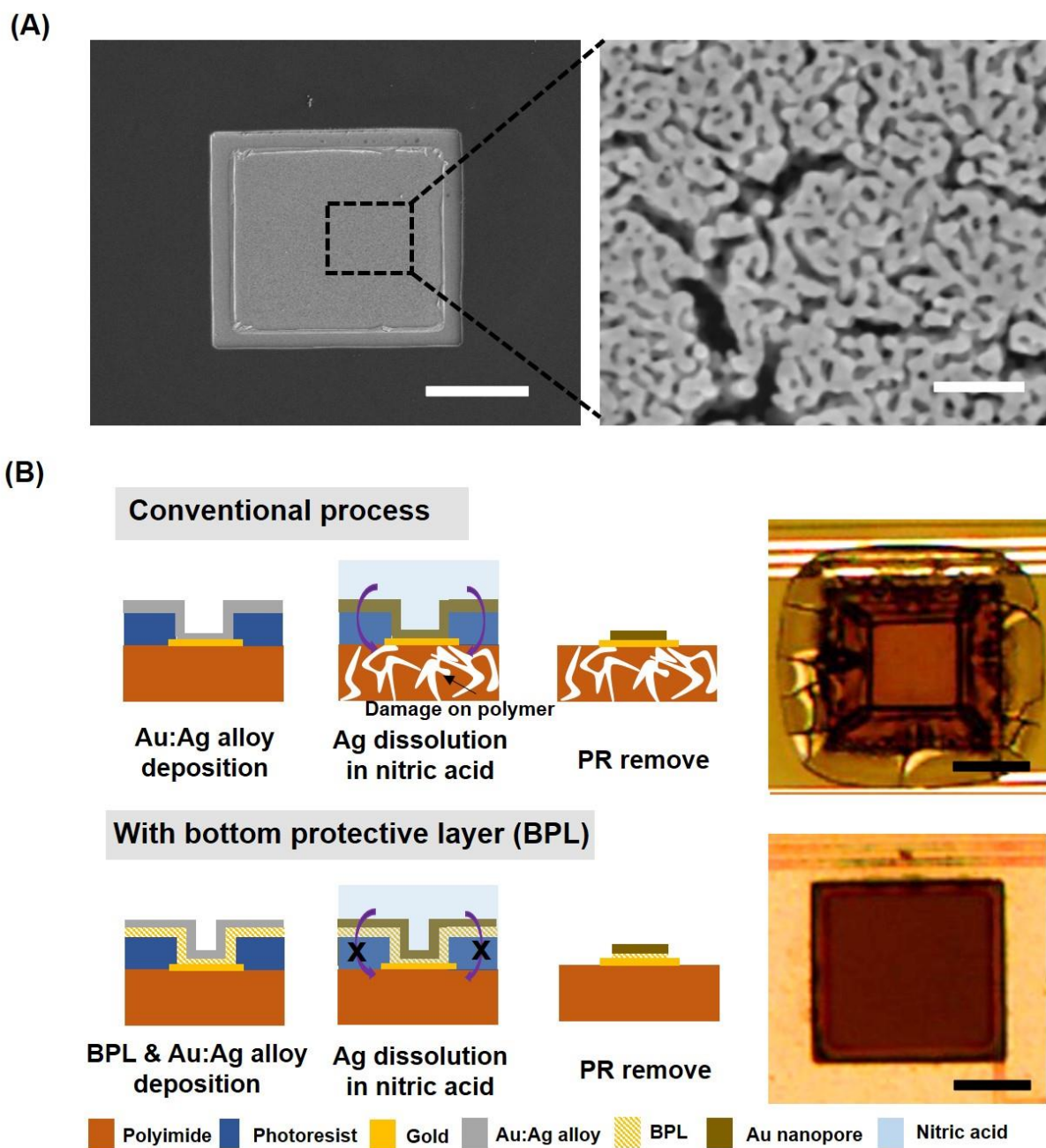


**Figure S3. Characterization of gold nanoporous microelectrodes.** (A) SEM image of  $100 \times 100 \mu\text{m}^2$  gold nanoporous microelectrodes and magnified image. Scale bar,  $50 \mu\text{m}$  (left) or  $50 \text{nm}$  (right). (B) Comparison of the conventional nitric acid dissolution process (top), which degrades the polyimide layer, versus a process that includes a bottom protective layer (BPL) to prevent damage to the polymer (bottom). Righthand panels show corresponding microscopic images of the resulting microelectrodes. Scale bar,  $50 \mu\text{m}$ .

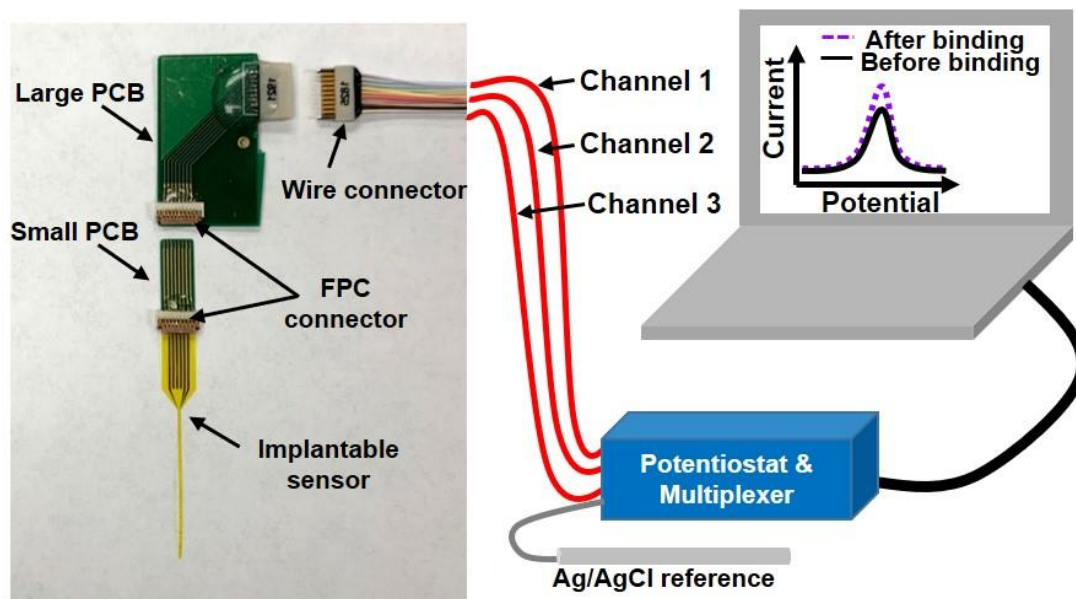


**Figure S4. The electrochemical measurement system used in this study.** The whole system includes the implantable sensor, FPC connector and printed circuit board (PCB) connection, and commercial potentiostat together with Ag/AgCl reference electrode, connected to a computer with custom Matlab code for real-time data processing and visualization. Photo Credit: Ji-Won Seo, Stanford University.

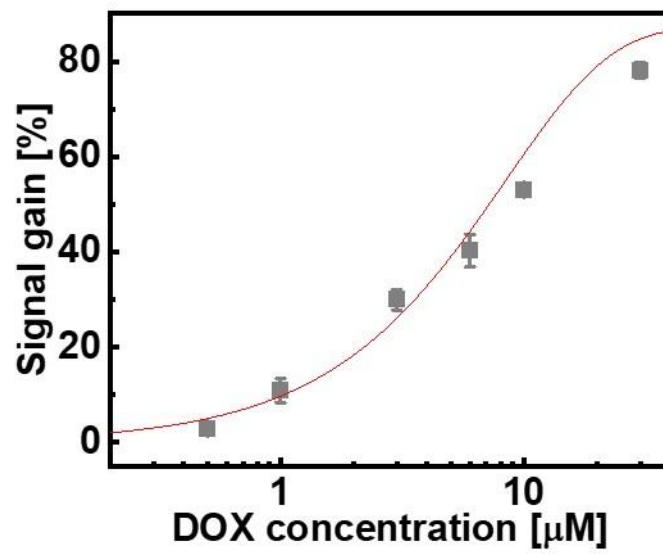


**Figure S5.** Calibration curve fitted to the average signal gain calculated from the multi-channel data shown in Figure 2B. Error bars were calculated from the three-channel data at each concentration.

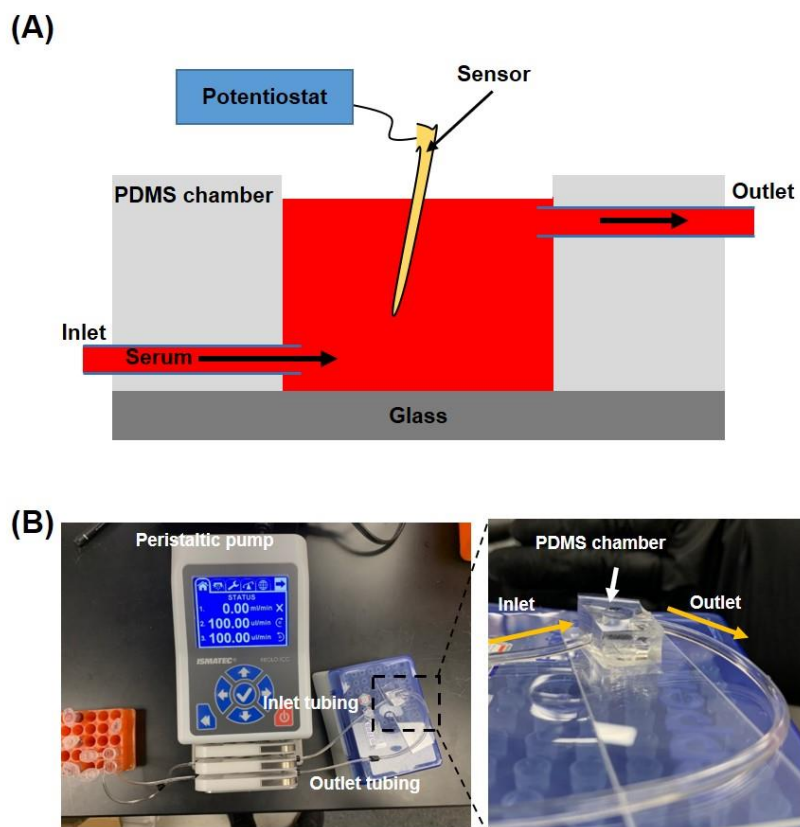


**Figure S6. Scheme (A) and photos (B) of the system used for testing our sensor in flowing serum.** Photo Credit: Ji-Won Seo, Stanford University.

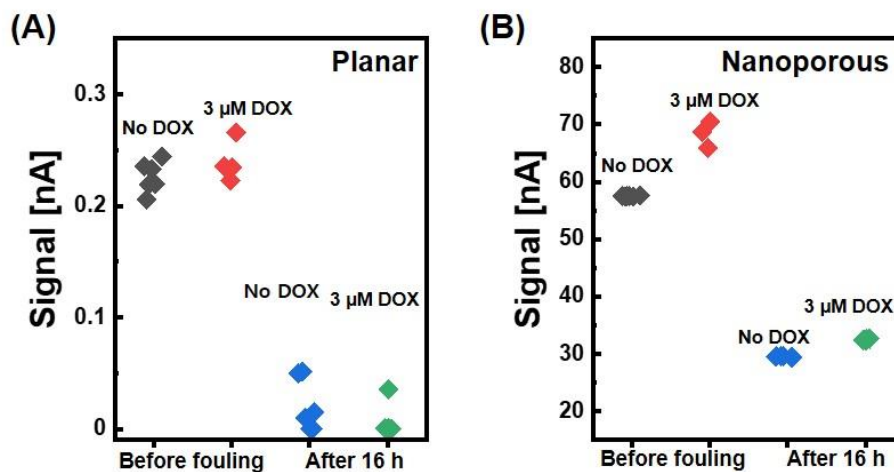


**Figure S7. Raw signal before and after spiking 3  $\mu\text{M}$  DOX into flowing serum for (A) planar and (B) nanoporous gold microelectrodes.** Data are shown for initial signal before biofouling can occur, and for signal obtained after 16 h in blood serum.



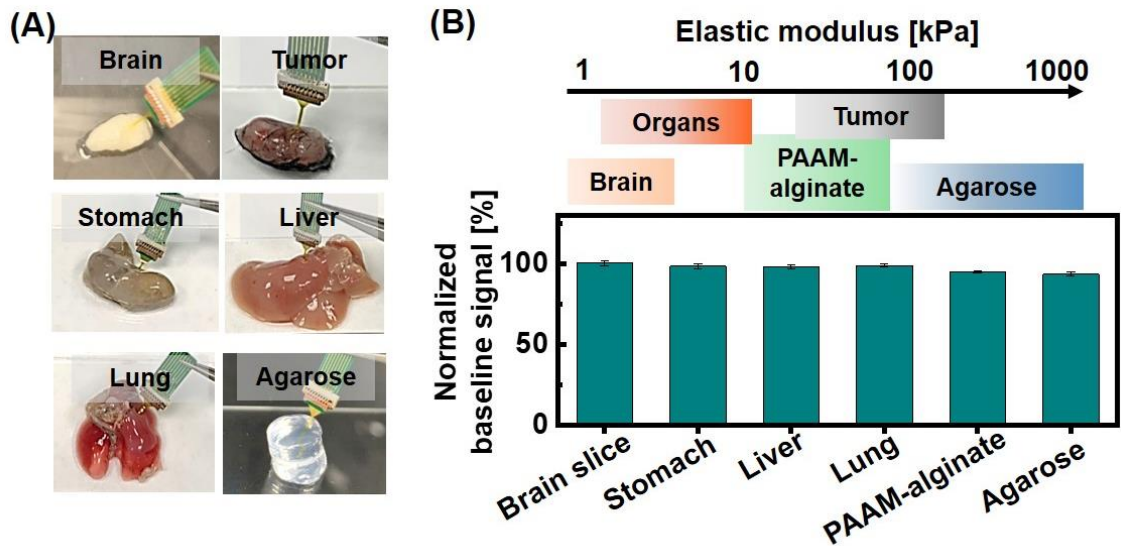


**Figure S8. The mechanical characterization of the nanoporous microelectrode device.** (A) Photos of our nanoporous microelectrode sensor inserted into various biological tissues or other materials and (B) the corresponding baseline signal change after 100 insertion cycles. These various materials reflect a broad range of elastic modulus values—the various biological tissues ranged from 1 to 100 kPa, and we also included PAAM-alginate hydrogel (30 kPa) and agarose hydrogel (1,000 kPa). Photo Credit: Ji-Won Seo, Stanford University.

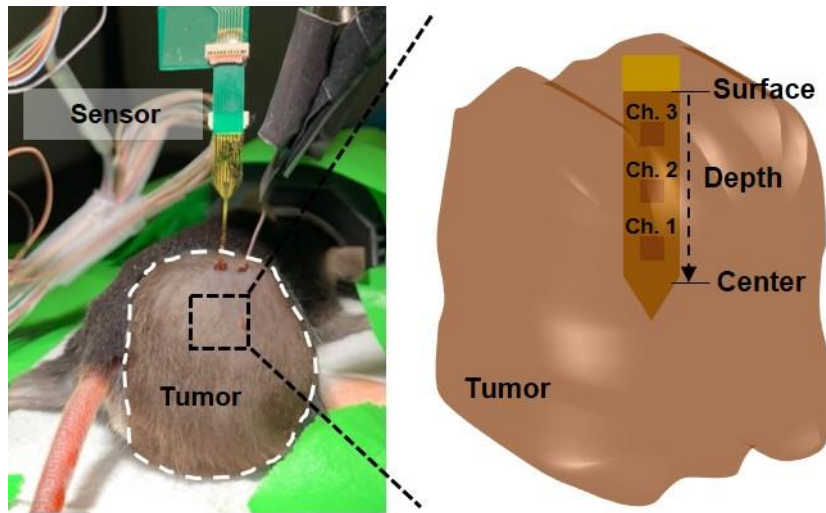


**Figure S9. Microelectrode array sensor implantation into tumor tissue of an anesthetized mouse.** Photo Credit: Ji-Won Seo, Stanford University.

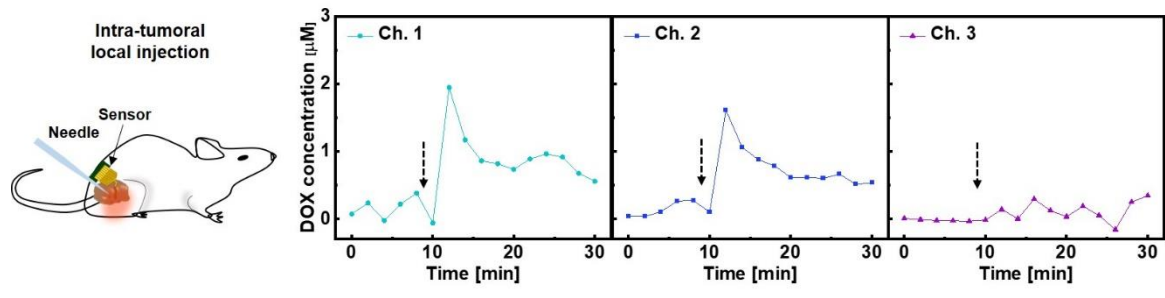


**Figure S10. Real-time DOX concentration measurements at each sensor channel after intra-tumoral injection of 10  $\mu\text{g/g}$  DOX near channel 1 at  $t = 9$  min (black dotted arrow).**

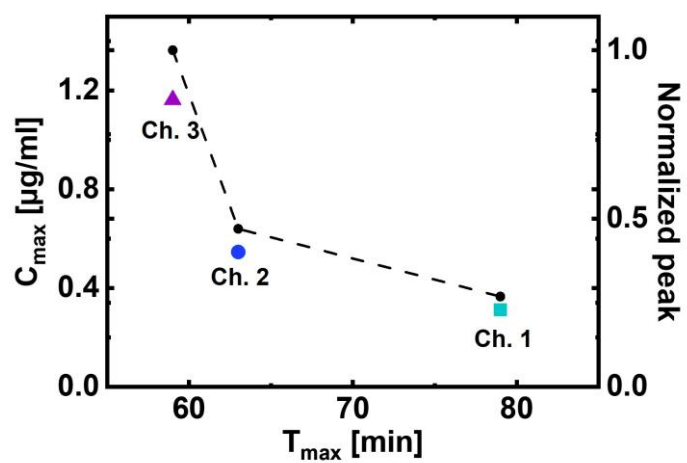


**Figure S11.** Maximum drug concentration ( $C_{max}$ , colored dots) and normalized peak (black dotted line) at the time at which  $C_{max}$  was reached ( $T_{max}$ ) at the three sensor channels.

**Table S1. Comparison of previous DOX measurements in tissue.**

<b>Works</b>	<b>Tumor model</b>	<b>Sacrificing animals</b>	<b>Sample preparation</b>	<b>Measurement type</b>	<b>DOX injection volume &amp; Max DOX concentration</b>
(57)	Orthotopic ovarian cancer	Multiple animals per each time point detection.	Tissue extraction, centrifuged, stored at 4°C, washing	Multiple time points, <i>Ex vivo</i>	10 µg/g DOX injection, 8 µg/g DOX in tumor
(58)	Tumor-free	Multiple animals per each time point detection.	Tissue extraction, centrifuged	Multiple time points, <i>Ex vivo</i>	5 µg/g DOX injection, 4 µg/g DOX in liver tissue
(59)	Tumor-free	Multiple animals per each time point detection.	Tissue extraction, centrifuged, stored overnight	Multiple time points, <i>Ex vivo</i>	12 µg/g DOX injection, ~2 µg/g DOX in muscle
<b>This work</b>	<b>Melanoma</b>	No	Don't need	Real-time, <i>In vivo</i>	10 µg/g DOX injection, ~1.05 µg/g DOX in tumor